

Investigation of pair-correlated 0^+ states in ^{134}Ba via the $^{136}\text{Ba}(p, t)$ reaction

J. C. Nzobadila Ondze,¹ B. M. Rebeiro^{1,*}, S. Triambak^{1,†}, L. Atar,² G. C. Ball³, V. Bildstein², C. Burbadge,² A. Diaz Varela,² T. Faestermann⁴, P. E. Garrett,^{2,1} R. Hertzenberger⁵, M. Kamil,¹ R. Lindsay¹, J. N. Orce¹, A. Radich,² and H.-F. Wirth⁵

¹*Department of Physics and Astronomy, University of the Western Cape, P/B X17, Bellville 7535, South Africa*

²*Department of Physics, University of Guelph, Guelph, Ontario N1G 2W1, Canada*

³*TRIUMF, 4004 Wesbrook Mall, Vancouver, British Columbia V6T 2A3, Canada*

⁴*Physik Department, Technische Universität München, D-85748 Garching, Germany*

⁵*Fakultät für Physik, Ludwig-Maximilians-Universität München, D-85748 Garching, Germany*



(Received 29 January 2021; accepted 17 March 2021; published 29 March 2021)

We performed a high resolution study of 0^+ states in ^{134}Ba using the $^{136}\text{Ba}(p, t)$ two-neutron transfer reaction. Our experiment shows a significant portion of the $L = 0$ pair-transfer strength concentrated at excited 0^+ levels in ^{134}Ba . Potential implications in the context of $^{136}\text{Xe} \rightarrow ^{136}\text{Ba}$ neutrinoless double beta decay matrix element calculations are briefly discussed.

DOI: [10.1103/PhysRevC.103.034329](https://doi.org/10.1103/PhysRevC.103.034329)

I. BACKGROUND

The even-mass barium isotopic chain ($Z = 56$) is a fertile testing ground for nuclear structure models and is also important for nuclear astrophysics studies and tests of fundamental symmetries. For example, theory calculations predict an enhanced octupole collectivity around ^{112}Ba , which is located on the $N = Z$ line [1,2]. Possible octupole correlations have been observed in the neutron-deficient ^{118}Ba [3] and ^{124}Ba [4] isotopes, while there is clear experimental evidence of octupole deformation in the ground states of neutron-rich Ba nuclei around $N = 88$ [5,6]. Furthermore, for $N \leq 82$, in the $A \approx 130$ region, the even Ba isotopes are expected to be shape transitional [7]. Their shape evolution ranges from nearly spherical (semimagic at $N = 82$) to γ -soft [8], where the shape changes are characterized by quantum phase transitions (QPTs) [9,10]. Within the interacting boson model (IBM), the ^{134}Ba isotope was identified as a potential E(5) symmetry critical point [11] for a second-order QPT. Independently, from a nuclear astrophysics perspective, fractional abundance ratios of odd-to-even barium isotopes as well as relative elemental ratios such as [Ba/Fe] and [Ba/Eu], etc., offer insight into the r and s -process neutron capture contributions [12,13] to heavy element nucleosynthesis in stellar environments. This is particularly relevant in metal-poor stars, where the dominant contribution to elemental abundances is expected to be from the r process [14]. One interesting example is the subgiant HD140283, in which case the fractional barium abundances obtained from independent spectral analyses have yielded inconsistent results. These discrepancies have stirred a debate

on the assumed r -process origin of the odd Ba isotopes during the early stages of galactic evolution [15–19].

In the context of fundamental symmetries, ^{136}Ba is the daughter nucleus in ^{136}Xe double beta decay, an attractive candidate to search for the lepton-number-violating neutrinoless double beta ($0\nu 2\beta$) transformation. Observation of such decays would unequivocally show that the neutrinos are their own antiparticles (i.e., they are Majorana fermions). In such a scenario, other useful information on lepton-number-violating new physics or the absolute neutrino mass scale, etc., can only be obtained if the nuclear matrix element (NME) for the decay is accurately known [20,21]. To this end, a variety of many-body techniques are used to evaluate $0\nu 2\beta$ decay NMEs in several candidate nuclei. These calculations have yielded significantly discrepant results for individual cases [20]. Addressing this apparent model dependence in all double beta decaying nuclei remains an important issue. We focus on this aspect here.

The dominant contribution to a $0\nu 2\beta$ decay NME arises from the transformation of nucleon pairs that couple to total angular momentum $J = 0$ [22–24]. Such a decay corresponds to spherical superfluid parent and daughter nuclei. The $J \neq 0$ contributions to the matrix element arise from higher seniority [22,23] components in the wave functions, due to broken Cooper pairs of nucleons. These lead to cancellations and effectively reduce the $0\nu 2\beta$ decay amplitude. An additional reduction in the NME is expected if there is a seniority mismatch between the initial and the final wave functions [25]. This would be the case if the parent and the daughter have different intrinsic shapes [26], that are driven by multipole correlations. It is now established that these collective correlations (other than pairing) play an important role in $0\nu 2\beta$ NME calculations [20] and could further quench calculated NMEs [26]. As examples, one can look at two traditionally used many-body methods, the interacting shell model (ISM)

*Present address: Université Lyon, Université Claude Bernard Lyon 1, CNRS/IN2P3, IP2I Lyon, UMR 5822, F-69622 Villeurbanne, France.

†striambak@uwc.ac.za

and the quasiparticle random phase approximation (QRPA). In the former, the treatment of correlations is exact, with comparatively smaller valence spaces. On the other hand, the QRPA calculations use larger model spaces, with relatively simpler configurations for the valence nucleons. Here, the pairing between like nucleons is treated via a transformation to the quasiparticle regime, within the Bardeen-Cooper-Schrieffer (BCS) approximation [27]. Such BCS pairing smears the Fermi surfaces in the parent and the daughter (as one would expect in a superfluid), while the RPA correlations admix higher seniority components in the wave functions [23,25]. In this context, (p, t) [28–31] and $({}^3\text{He}, n)$ [32] two-nucleon transfer experiments offer valuable insight into pairing correlations between like nucleons [33]. For reactions on even-even nuclei, strong population of the ground states (relative to excited 0^+ states) would imply that both the target and residual nucleus ground states are nearly superfluid, and well described by BCS wave functions [28,33].

For the case of ${}^{136}\text{Xe} \rightarrow {}^{136}\text{Ba}$, the $0\nu 2\beta$ decay NME differs more than a factor of 4, depending on the many-body technique used [34]. This is an important issue as ${}^{136}\text{Xe}$ decay is a promising candidate to search for $0\nu 2\beta$ decays [34]. In fact, several planned large-scale time projection chamber (TPC) based experiments aim to measure ${}^{136}\text{Xe}$ $0\nu 2\beta$ decay [35–38]. From a nuclear structure perspective this is an interesting case, because of its location in a shape-transitional region of the Segrè chart. While the nearly spherical ${}^{136}\text{Xe}$ has a closed shell at $N = 82$, the daughter ${}^{136}\text{Ba}$ has $N = 80$.

In light of the above, we recently benchmarked the $J = 0$ part of the ${}^{136}\text{Xe}$ $0\nu 2\beta$ decay NME, via a study of neutron pairing correlations using the ${}^{138}\text{Ba}(p, t)$ reaction [34]. Contrary to what one would expect for spherical superfluid systems [33], we observed for the first time a strong population of higher lying 0^+ states, relative to the ground state in ${}^{136}\text{Ba}$. About 53% of the ground state $L = 0$ (p, t) strength was distributed over excited 0^+ states, with $\approx 35\%$ concentrated at the 0_2^+ , 0_3^+ , and 0_4^+ levels. This was clear evidence of a breakdown of the BCS approximation for neutrons in ${}^{136}\text{Ba}$. The results also implied significantly different ground state wave functions for the spherical ${}^{138}\text{Ba}$ and the (final-state) ${}^{136}\text{Ba}$ nucleus. If this were the case, because one can expect nearly identical ground state wave functions for the $N = 82$ ${}^{138}\text{Ba}$ and ${}^{136}\text{Xe}$ nuclei, a sizable difference in deformation (seniority mismatch) between the parent and the daughter in ${}^{136}\text{Xe} \rightarrow {}^{136}\text{Ba}$ $\beta\beta$ decay cannot be ruled out.

Further investigations of shape-transitional barium isotopes around $A = 130$ are relevant in the context of the above. Previous data from (p, t) reactions on barium isotopes show inconclusive evidence in this regard. For the ${}^{136}\text{Ba}(p, t)$ case, Cata-Danil *et al.* [39] observe around 34% of the ground state strength distributed over excited 0^+ states in ${}^{134}\text{Ba}$. However their measured $L = 0$ strength distribution was around a factor of 2 larger than what was reported in subsequent work by Pascu *et al.* [40]. Similarly, for the ${}^{134}\text{Ba}(p, t)$ reaction, Ref. [39] reports $\approx 27\%$ of the ground state strength distributed over excited 0^+ states, while Ref. [40] claims this value is much smaller, at around 10%. Adequate ${}^{136}\text{Ba}(p, t)$ angular distribution data were not presented in both references. In comparison, measured ${}^{132,130}\text{Ba}(p, t)$ cross sections

do not show a similar fragmentation of the monopole strength [41,42].

Considering the aforementioned discrepancies and given the importance of the measured results, in this paper we report remeasurements of the relative population of 0^+ states in ${}^{134}\text{Ba}$, with the ${}^{136}\text{Ba}(p, t)$ reaction.

II. EXPERIMENTAL DETAILS

The experiment was performed at the Maier-Leibnitz-Laboratorium (MLL), operated jointly by the Ludwig-Maximilian Universität (LMU) and Technische Universität München (TUM), in Garching, Germany. 22 MeV protons from the MLL tandem accelerator were directed onto a $40 \mu\text{g}/\text{cm}^2$, 93% isotopically enriched ${}^{136}\text{BaO}$ target, that was evaporated on a thin carbon foil. The light reaction products were momentum analyzed with the high-resolution Q3D magnetic spectrograph [43,44]. The focal plane detector for the spectrograph comprised two gas proportional counters and a 7-mm-thick plastic scintillator [44]. The energy losses of the charged ejectiles in the proportional counters and the residual energy deposited in the plastic scintillator were used to discriminate the tritons from other ejectiles (as shown in Fig. 1). A cathode strip foil in the second proportional counter provided high-resolution position information for the tritons.

We collected triton spectra at five magnetic field settings and at ten angles, ranging from 5° to 50° (in 5° increments). The Q3D field settings allowed us to study states in ${}^{134}\text{Ba}$ up to around 4 MeV in excitation energy, with full widths at half maximum of $\lesssim 10$ keV for the triton peaks. The triton energies were calibrated *in situ*, using well known states in ${}^{134}\text{Ba}$ [48]. A sample spectrum is shown in Fig. 2.

During the course of the experiment, we also collected ${}^{136}\text{Ba}(p, p)$ data over an angular range of 10° – 60° . These data allowed us to accurately determine the effective ${}^{136}\text{Ba}$ areal density in the target foil, from small angle scattering. Additionally, both the (p, p) and the (p, t) data sets from this work were analyzed as described in Ref. [34], given the similarity between the two experiments.

III. ANALYSIS

We performed distorted wave Born approximation (DWBA) calculations of angular distributions using the DWUCK4 code [49] and compared them to our experimental results. The DWBA analysis used Woods-Saxon potentials and global optical model potential (OMP) parameters. Based on the agreement with our measured ${}^{136}\text{Ba}(p, p)$ cross sections and a comparison with previous ${}^{138}\text{Ba}(p, p)$ data obtained over a large angular range [34], we chose the global OMP parameters recommended by Varner *et al.* [50] for the incoming proton channel in the DWUCK4 calculations. For the triton channel we chose the OMPs recommended by Li, Liang, and Cai [45], as they yielded better agreement with our measured ground state angular distribution for ${}^{134}\text{Ba}$. This is shown in Fig. 3. The two-neutron transfer form factor was obtained using the OMPs from Ref. [51], assuming a $(0h_{11/2})^2$ configuration [52] for the form factor. For each

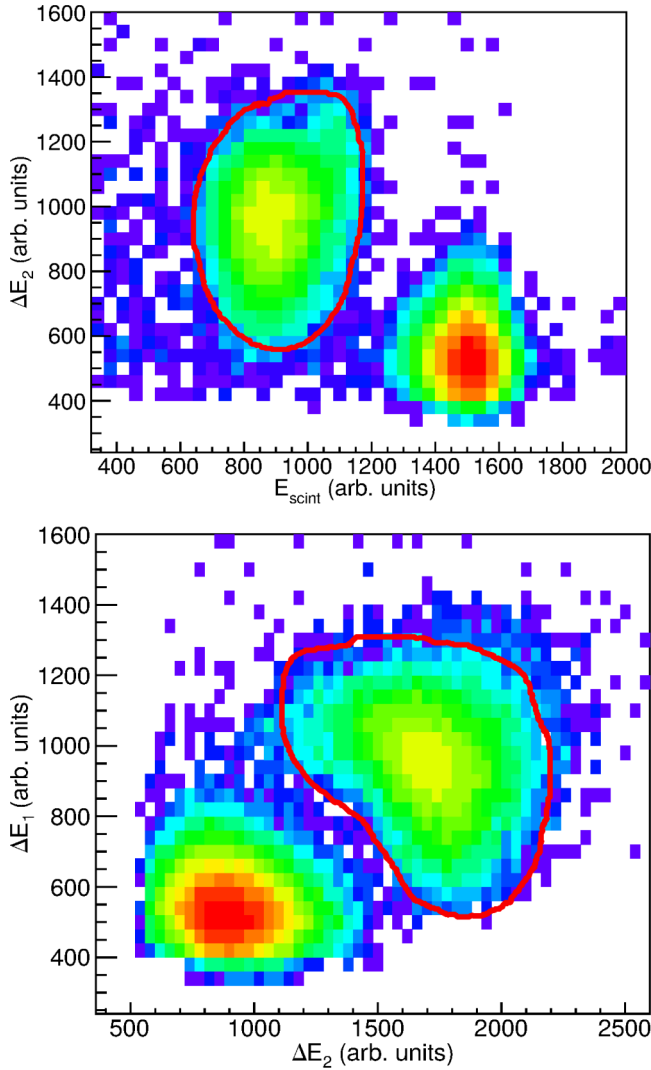


FIG. 1. Particle identification spectra using energy losses registered in the two proportional counters and the total energy deposited in the plastic scintillator. The triton groups are highlighted. The other particles are mainly deuterons.

state, the depth of the potential was adjusted such that each transferred neutron had a binding energy $(S_{2n} + E_x)/2$, where S_{2n} is the two neutron separation energy of ^{136}Ba and E_x is the excitation energy in the residual ^{134}Ba nucleus.

The above DWBA prescription was used to perform an angular distribution analysis of all the peaks shown in Fig. 2, that corresponded to states in ^{134}Ba . We identify seven 0^+ states in ^{134}Ba . These include the ground state and a previously unreported level at 3528 keV.¹ The measured angular distributions are shown in Fig. 4. These data determined the monopole (p, t) strengths for excited 0^+ states, relative to the ground state. This was done using the ratio [34]

$$\epsilon_i = \left[\frac{\left(\frac{d\sigma}{d\Omega}\right)_{0^+ \text{ex}}^{\text{data}}}{\left(\frac{d\sigma}{d\Omega}\right)_{0^+ \text{ex}}^{\text{DWBA}}} \right]_i \left[\frac{\left(\frac{d\sigma}{d\Omega}\right)_{\text{G.S.}}^{\text{DWBA}}}{\left(\frac{d\sigma}{d\Omega}\right)_{\text{G.S.}}^{\text{data}}} \right], \quad (1)$$

¹An independent confirmation of this state would be welcome.

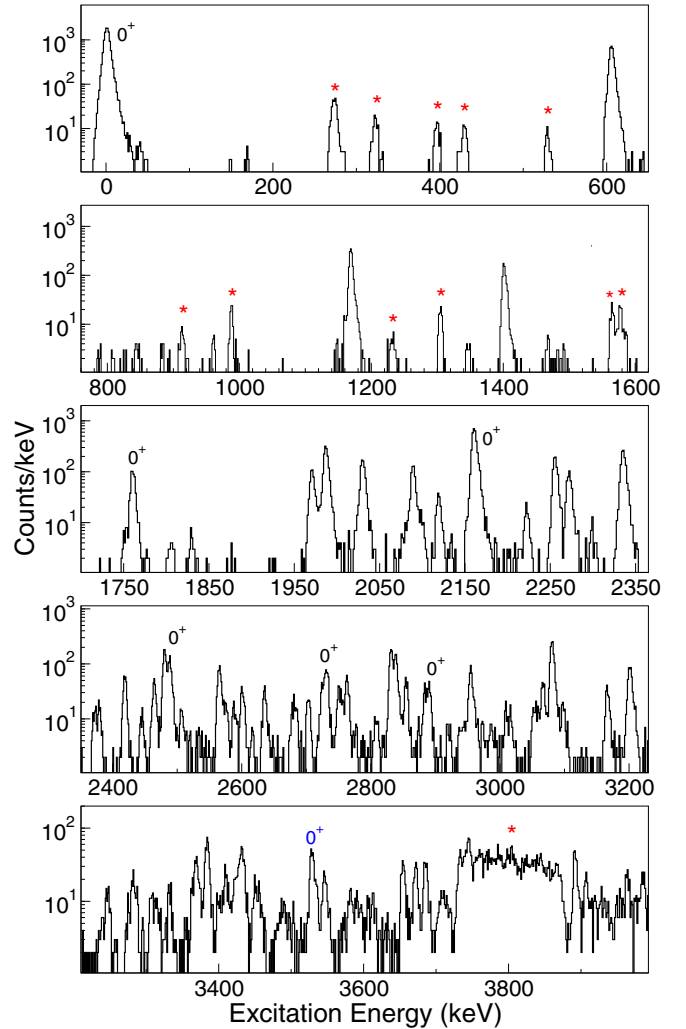


FIG. 2. Triton spectra corresponding to states in ^{134}Ba , obtained at $\theta_{\text{lab}} = 25^\circ$. Peaks from contaminants in the target are marked with asterisks. The 0^+ states observed in this experiment are labeled. The state at 3528 keV (labeled in blue) is reported for the first time in this work.

which removed any Q value dependence on the differential cross sections.

The results are shown in Table I. We find that our extracted value for the *integrated strength* is more consistent with the result of Cata-Danil *et al.* [39] and disagrees significantly with the later work of Pascu *et al.* [40]. We also observe large discrepancies between our work and Ref. [40] for individual states, and identify fewer excited 0^+ states than either of these measurements.² A few aspects of this comparison are discussed below.

The Nuclear Data Sheets (NDS) for $A = 134$ [53] list a doublet of states at 2334.76(6) and 2336.82(3) keV. These levels are assigned spin-parity $(1, 2^+)$ and 0^+ respectively. The Q3D spectrograph (also used in Refs. [39,40]) is limited by

²The results of Refs. [39,40] are also discordant with one another, for both $^{136,134}\text{Ba}(p, t)$ data.

TABLE I. Measured $L = 0$ $^{136}\text{Ba}(p, t)$ strength distribution over excited 0^+ states in ^{134}Ba , relative to the ground state.^a For comparison we also list the results from previous work [39,40] and our measured differential cross sections at $\theta_{\text{lab}} = 5^\circ$.

| Ref. [39] | | Ref. [40] | | This work ^b | | $(d\sigma/d\Omega)_{5^\circ}$ |
|--------------------------|---------------------|-------------------------------|---------------------|-------------------------------|---------------------|-------------------------------|
| E_x (keV) | ϵ_i (%) | E_x (keV) | ϵ_i (%) | E_x (keV) | ϵ_i (%) | This work |
| 0.0 | 100.0 | 0.0 | 100.0 | 0.0 | 100.0 | 3.5(1) |
| 1759 | 3.73 | 1760.8(3) | 2.6(1) | 1760.3(3) | 10.3(4) | 0.185(7) |
| 2161 | 14.85 | 2159.1(2) | 8.8(3) | 2159.6(3) | 16.6(5) | 0.225(8) |
| 2336 | ≤ 1.05 | | | 2334.2(3) | ≤ 3.0 | 0.028(2) |
| 2378 | 0.52 | 2380.7(9) ^c | 0.10(1) | 2379.0(4) | ≤ 0.5 | 0.004(1) |
| 2485 | 6.67 | 2488.6(1) | 2.2(1) | 2488.4(3) | 8.3(4) | 0.076(4) |
| 2722 | 1.99 | 2727.5(2) | 1.0(1) | 2729.0(4) | 5.5(3) | 0.028(2) |
| 2874 | 1.81 | 2883.8(2) | 0.8(1) | 2887.0(5) | 2.6(2) | 0.016(2) |
| | | 2961.1(12) ^c | 0.10(1) | | | |
| 2996 | 0.63 | 3000.6(2) | 0.3(1) | | | |
| 3181 | 1.40 | | | | | |
| | | 3395.1(10) | 0.10(1) | | | |
| 3501 | 1.47 | 3505.4(5) | 0.5(1) | | | |
| | | | | 3528(1) | 1.6(2) | 0.004(1) |
| | | 3602.3(11) ^c | 0.10(1) | | | |
| 3618 | 1.22 | 3623.9(4) ^c | 0.4(1) | | | |
| | | 3750.4(10) ^c | 0.2(1) | | | |
| $\sum \epsilon_i = 34\%$ | | $\sum \epsilon_i = 17.1(4)\%$ | | $\sum \epsilon_i = 44.9(9)\%$ | | |

^aThe 0^+ assignments for states above 2488 keV were only made from $^{136}\text{Ba}(p, t)$ measurements.

^bAs in Ref. [39], we also note that the configurations other than $(0h_{11/2})^2$ yield similar results.

^cThese states were tentatively assigned spin-parity $J^\pi = (0^+)$.

energy resolution to differentiate between these two states. We observe a single triton peak corresponding to $E_x = 2334.2(3)$ keV, which has an angular distribution that is more consistent with an $L = 2$ transition.³ This indicates that the population of the 2337 keV level was below our experimental sensitivity. We encounter a similar situation at about 2.4 MeV, with two known closely spaced states at 2379.112(18) keV [53] and 2377.1(4) keV [53,54]. The former is an established 0^+ level, while the latter was assigned a tentative spin value of $J = (6)$ [53]. Our spectrum shows a triton peak corresponding to 2379.0(4) keV, whose measured angular distribution agrees well with $L = 2$ transfer.

As a result of the above, we measured cross sections at 5° to place upper limits the $L = 0$ strengths for the 2337 and 2379 keV levels. Several of the other weakly populated 0^+ states reported at higher excitation energies in Refs. [39,40] were not observed in this work. A probable explanation for this can be invoked from the fact that the previous measurements were carried out at a higher beam energy of 25 MeV. Due to the large negative Q value for this reaction (-7.6 MeV), the $L = 0$ cross section at the most forward angles decreases more rapidly with increase in excitation energy for 22 MeV protons as compared to 25 MeV. Our DWBA calculations show that at 22 MeV the forward angle differential cross sections are around a factor of 2 smaller at 1.8 MeV excitation energy, compared to those at 25 MeV. This factor increases

to approximately 5 and 10 at excitation energies of 2.5 and 3.5 MeV, respectively. In contrast, large changes in forward angle differential cross sections are not predicted for $L = 2$ transitions (for example).

It is difficult to comment further since both Refs. [39,40] reported meager $^{136}\text{Ba}(p, t)$ angular distribution data. Catalani *et al.* [39] acquired data at only two angles and chose to identify the $L = 0$ transitions using a single number, the

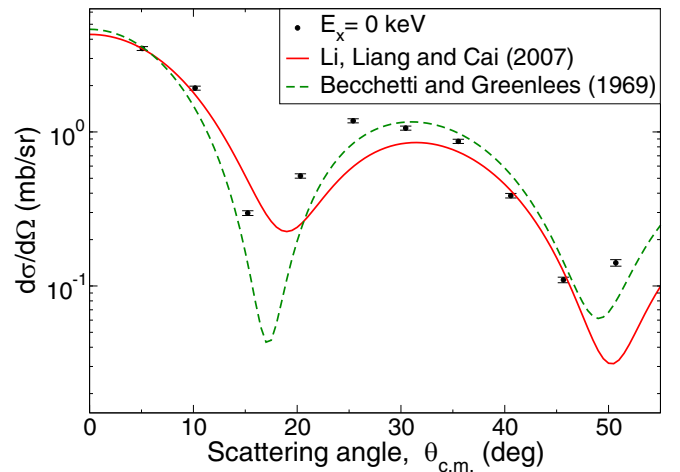


FIG. 3. Measured ^{134}Ba ground state angular distribution compared with normalized DWBA predictions obtained using different triton OMPs by Li, Liang, and Cai (2007) [45] and Becchetti and Greenlees (1969) [46,47].

³A detailed analysis of the full data set will be presented in a future publication.

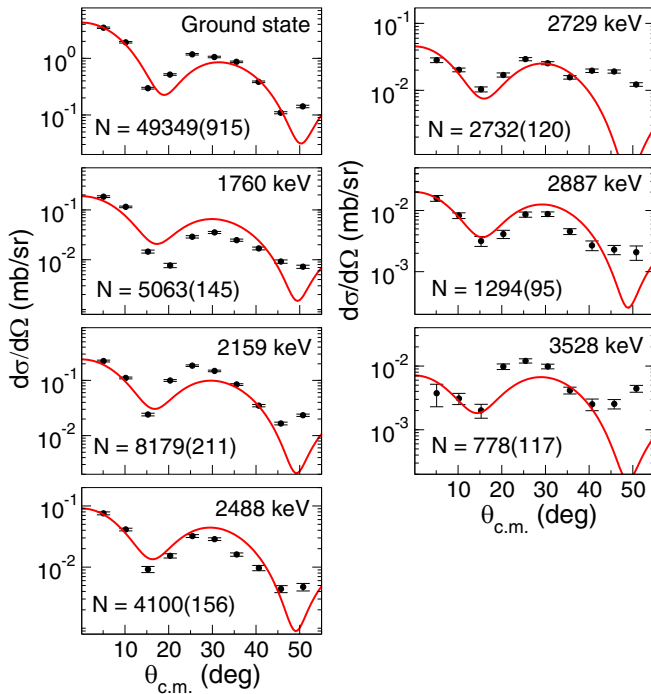


FIG. 4. $^{136}\text{Ba}(p, t)$ angular distributions for observed 0^+ states in ^{134}Ba , compared with normalized DWBA predictions for $L = 0$ transfer. The DWBA results are obtained using the $(0h_{11/2})^2$ configuration for the form factor and normalized such that $(d\sigma/d\Omega)_{\text{expt}} = N(d\sigma/d\Omega)_{\text{DWBA}}$.

ratio of the cross sections at $\theta_{\text{lab}} = 6^\circ$ and 15° . In comparison, Pascu *et al.* acquired data at only three angles [40] and do not explicitly show angular distributions for excited 0^+ states. They identified the 0^+ states using the same procedure as in Ref. [39]. Adequate descriptions regarding the choice of OMP parameters for their analyses and the procedure to determine target thicknesses were not provided in these references. However, since both these works provided more complete $^{134}\text{Ba}(p, t)$ angular distribution plots, we are able to address the discrepancy for this reaction. In particular, our estimated values of ϵ_i (via inspection and from DWBA calculations) show better agreement with the results of Ref. [39] and

significantly disagree with the results in Ref. [40]. This gives credence to the former [39] $^{136,134}\text{Ba}(p, t)$ results over the latter [40].

IV. CONCLUSIONS

It is evident from our results in Table I that a significant portion of the (p, t) strength is distributed over excited 0^+ levels in ^{134}Ba . This is similar to our previously reported $^{138}\text{Ba}(p, t)$ results [34] and clearly indicates a breakdown of the BCS approximation for neutrons in ^{134}Ba . The persistence of such behavior as one moves away from the $N = 82$ shell closure, with integrated $^{138,136,134}\text{Ba}(p, t)$ strengths being $\approx 53\%$, 45% , and 27% highlights the shape-transitional nature of these isotopes. This observed systematic trend implies significantly different deformations in the ground states of ^{138}Ba , ^{136}Ba , and ^{134}Ba and a mismatch between the initial and final states in ^{136}Xe $\beta\beta$ decay. Such a curtailed overlap between the parent and daughter wave functions would explain the anomalously long $2\nu 2\beta$ decay half-life measured for ^{136}Xe [55,56], compared to other candidates [57]. As $2\nu 2\beta$ decay is the ultimate irreducible background in any neutrinoless double beta decay experiment, the long half-life offers ^{136}Xe $\beta\beta$ experiments a unique advantage in terms of achieving a better signal-to-noise ratio [58]. On the other hand, such overlap mismatch would also reduce the calculated ^{136}Xe $0\nu 2\beta$ decay NME, compared to a scenario in which both the parent and daughter are nearly spherical (or similarly deformed). Both experimental investigations of quadrupole correlations in ^{136}Ba as well as theoretical studies of deformation effects on the NME (along the lines of Refs. [59,60]) will be useful to further shed light in this regard. A potential starting point for the former may be the remeasurement of the spectroscopic quadrupole moment of the first 2^+ state in ^{136}Ba , for which discrepant values exist in the literature [61–63].

ACKNOWLEDGMENTS

This work was partially funded by the National Research Foundation (NRF), South Africa under Grant No. 85100. J.C.N.O thanks the NRF funded MaNuS/MatSci program at UWC for financial support during the course of his M.Sc.

- [1] J. Skalski, *Phys. Lett. B* **238**, 6 (1990).
- [2] P.-H. Heenen, J. Skalski, P. Bonche, and H. Flocard, *Phys. Rev. C* **50**, 802 (1994).
- [3] J. F. Smith *et al.*, *Phys. Rev. C* **57**, R1037 (1998).
- [4] P. Mason *et al.*, *Phys. Rev. C* **72**, 064315 (2005).
- [5] B. Bucher *et al.*, *Phys. Rev. Lett.* **116**, 112503 (2016).
- [6] B. Bucher *et al.*, *Phys. Rev. Lett.* **118**, 152504 (2017).
- [7] E. Marshalek, L. W. Person, and R. K. Sheline, *Rev. Mod. Phys.* **35**, 108 (1963).
- [8] R. Casten and P. Von Brentano, *Phys. Lett. B* **152**, 22 (1985).
- [9] P. Cejnar, J. Jolie, and R. F. Casten, *Rev. Mod. Phys.* **82**, 2155 (2010).
- [10] K. Nomura, T. Nikšić, and D. Vretenar, *Phys. Rev. C* **96**, 014304 (2017).
- [11] R. F. Casten and N. V. Zamfir, *Phys. Rev. Lett.* **85**, 3584 (2000).
- [12] L. Mashonkina and T. Gehren, *Astron. Astrophys.* **364**, 249 (2000).
- [13] T. Tsujimoto, T. Shigeyama, and Y. Yoshii, *Astrophys. J.* **531**, L33 (2000).
- [14] J. W. Truran, *Astron. Astrophys.* **97**, 391 (1981).
- [15] A. J. Gallagher, S. G. Ryan, A. E. García Pérez, and W. Aoki, *Astron. Astrophys.* **523**, A24 (2010).
- [16] P. Magain, *Astron. Astrophys.* **297**, 686 (1995).
- [17] P. François, *Astron. Astrophys.* **313**, 229 (1996).
- [18] R. Collet, M. Asplund, and P. E. Nissen, *Pub. Astron. Soc. Aust.* **26**, 330 (2009).
- [19] D. L. Lambert and C. Allende Prieto, *Mon. Not. R. Astron. Soc.* **335**, 325 (2002).

- [20] J. Engel and J. Menéndez, *Rep. Prog. Phys.* **80**, 046301 (2017).
- [21] H. Ejiri, J. Suhonen, and K. Zuber, *Phys. Rep.* **797**, 1 (2019).
- [22] E. Caurier, J. Menéndez, F. Nowacki, and A. Poves, *Phys. Rev. Lett.* **100**, 052503 (2008).
- [23] F. Šimkovic, A. Faessler, V. Rodin, P. Vogel, and J. Engel, *Phys. Rev. C* **77**, 045503 (2008).
- [24] Y. Iwata, N. Shimizu, T. Otsuka, Y. Utsuno, J. Menéndez, M. Honma, and T. Abe, *Phys. Rev. Lett.* **116**, 112502 (2016).
- [25] E. Caurier, F. Nowacki, and A. Poves, *Eur. Phys. J. A* **36**, 195 (2008).
- [26] A. Poves, in *Fifty Years of Nuclear BCS*, edited by R. A. Broglia and V. Zelevinsky (World Scientific, Singapore, 2013), pp. 297–308.
- [27] F. T. Avignone, S. R. Elliott, and J. Engel, *Rev. Mod. Phys.* **80**, 481 (2008).
- [28] S. J. Freeman, J. P. Schiffer, A. C. C. Villari, J. A. Clark, C. Deibel, S. Gros, A. Heinz, D. Hirata, C. L. Jiang, B. P. Kay, A. Parikh, P. D. Parker, J. Qian, K. E. Rehm, X. D. Tang, V. Werner, and C. Wrede, *Phys. Rev. C* **75**, 051301(R) (2007).
- [29] T. Bloxham, B. P. Kay, J. P. Schiffer, J. A. Clark, C. M. Deibel, S. J. Freeman, S. J. Freedman, A. M. Howard, S. A. McAllister, P. D. Parker, D. K. Sharp, and J. S. Thomas, *Phys. Rev. C* **82**, 027308 (2010).
- [30] J. S. Thomas, S. J. Freeman, C. M. Deibel, T. Faestermann, R. Hertenberger, B. P. Kay, S. A. McAllister, A. J. Mitchell, J. P. Schiffer, D. K. Sharp, and H.-F. Wirth, *Phys. Rev. C* **86**, 047304 (2012).
- [31] D. K. Sharp, S. J. Freeman, B. D. Cropper, P. J. Davies, T. Faestermann, T. M. Hatfield, R. Hertenberger, S. J. F. Hughes, P. T. MacGregor, and H.-F. Wirth, *Phys. Rev. C* **100**, 024329 (2019).
- [32] A. Roberts, A. M. Howard, J. J. Kolata, A. N. Villano, F. D. Becchetti, P. A. De Young, M. Febraro, S. J. Freeman, B. P. Kay, S. A. McAllister, A. J. Mitchell, J. P. Schiffer, J. S. Thomas, and R. O. Torres-Isea, *Phys. Rev. C* **87**, 051305(R) (2013).
- [33] R. A. Broglia, O. Hansen, and C. Riedel, in *Advances in Nuclear Physics: Volume 6*, edited by M. Baranger and E. Vogt (Springer, Boston, 1973), pp. 287–457.
- [34] B. M. Rebeiro, S. Triambak, P. E. Garrett, B. A. Brown, G. C. Ball, R. Lindsay, P. Adsley, V. Bildstein, C. Burbadge, A. Diaz Varela, T. Faestermann, D. L. Fang, R. Hertenberger, M. Horoi, B. Jigmeddorj, M. Kamil, K. G. Leach, P. Z. Mabika, J. C. Nzubadila Ondze, J. N. Orce, and H.-F. Wirth, *Phys. Lett. B* **809**, 135702 (2020).
- [35] J. B. Albert *et al.* (nEXO Collaboration), *Phys. Rev. C* **97**, 065503 (2018).
- [36] D. S. Akerib *et al.* (LUX-ZEPLIN Collaboration), *Phys. Rev. C* **102**, 014602 (2020).
- [37] F. Agostini *et al.* (DARWIN Collaboration), *Eur. Phys. J. C* **80**, 808 (2020).
- [38] J. J. Gomez-Cadenas, in *37th International Conference on High Energy Physics (ICHEP)* [*Nucl. Part. Phys. Proc.* **273-275**, 1732 (2016)].
- [39] G. Cata-Danil, D. Bucurescu, L. Trache, A. M. Oros, M. Jaskola, A. Gollwitzer, D. Hofer, S. Deylitz, B. D. Valnion, and G. Graw, *Phys. Rev. C* **54**, 2059 (1996).
- [40] S. Pascu, G. Cata-Danil, D. Bucurescu, N. Mărginean, C. Müller, N. V. Zamfir, G. Graw, A. Gollwitzer, D. Hofer, and B. D. Valnion, *Phys. Rev. C* **81**, 014304 (2010).
- [41] S. Pascu, G. Cata-Danil, D. Bucurescu, N. Mărginean, N. V. Zamfir, G. Graw, A. Gollwitzer, D. Hofer, and B. D. Valnion, *Phys. Rev. C* **79**, 064323 (2009).
- [42] G. Suliman, D. Bucurescu, R. Hertenberger, H. F. Wirth, T. Faestermann, R. Krücken, T. Behrens, V. Bildstein, K. Eppinger, C. Hinke, M. Mahgoub, P. Meierbeck, M. Reithner, S. Schwertel, and N. Chauvin, *Eur. Phys. J. A* **36**, 243 (2008).
- [43] M. Löffler, H. Scheerer, and H. Vonach, *Nucl. Instrum. Methods* **111**, 1 (1973).
- [44] G. Dollinger and T. Faestermann, *Nucl. Phys. News* **28**, 5 (2018).
- [45] X. Li, C. Liang, and C. Cai, *Nucl. Phys. A* **789**, 103 (2007).
- [46] R. Capote *et al.*, *Nucl. Data Sheets* **110**, 3107 (2009), Special Issue on Nuclear Reaction Data.
- [47] <https://www-nds.iaea.org/RIPL-3/>.
- [48] <http://www.nndc.bnl.gov/ensdf/>.
- [49] P. D. Kunz, DWUCK4 DWBA Program, University of Colorado, 1978 (unpublished).
- [50] R. Varner, W. Thompson, T. McAbee, E. Ludwig, and T. Clegg, *Phys. Rep.* **201**, 57 (1991).
- [51] F. D. Becchetti and G. W. Greenlees, *Phys. Rev.* **182**, 1190 (1969).
- [52] S. V. Szewc, B. P. Kay, T. E. Cocolios, J. P. Entwisle, S. J. Freeman, L. P. Gaffney, V. Guimarães, F. Hammache, P. P. McKee, E. Parr, C. Portail, J. P. Schiffer, N. de Séréville, D. K. Sharp, J. F. Smith, and I. Stefan, *Phys. Rev. C* **94**, 054314 (2016).
- [53] A. A. Sonzogni, *Nucl. Data Sheets* **103**, 1 (2004).
- [54] B. Fazekas, T. Belgya, G. Molnár, Á. Veres, R. Gatenby, S. Yates, and T. Otsuka, *Nucl. Phys. A* **548**, 249 (1992).
- [55] N. Ackerman *et al.* (EXO Collaboration), *Phys. Rev. Lett.* **107**, 212501 (2011).
- [56] A. Gando *et al.* (KamLAND-Zen Collaboration), *Phys. Rev. C* **85**, 045504 (2012).
- [57] R. Saakyan, *Annu. Rev. Nucl. Part. Sci.* **63**, 503 (2013).
- [58] M. J. Dolinski, A. W. Poon, and W. Rodejohann, *Annu. Rev. Nucl. Part. Sci.* **69**, 219 (2019).
- [59] P. K. Rath, R. Chandra, K. Chaturvedi, P. K. Raina, and J. G. Hirsch, *Phys. Rev. C* **80**, 044303 (2009).
- [60] D.-L. Fang, A. Faessler, V. Rodin, and F. Šimkovic, *Phys. Rev. C* **83**, 034320 (2011).
- [61] J. R. Kerns and J. X. Saladin, *Phys. Rev. C* **6**, 1016 (1972).
- [62] M. J. Bechara, O. Dietzsch, and J. H. Hirata, *Phys. Rev. C* **29**, 1672 (1984).
- [63] P. J. Rothschild, A. M. Baxter, S. M. Burnett, M. P. Fewell, G. J. Gyapong, and R. H. Spear, *Phys. Rev. C* **34**, 732 (1986).